

Quantum confinement effects on the ordering of the lowest-lying excited states in conjugated polymers

Z. Shuai ^a, J.L. Brédas ^a, S. K. Pati ^b, and S. Ramasesha ^b

^aService de Chimie des Matériaux Nouveaux,
Centre de Recherche en Electronique et Photonique Moléculaires,
Université de Mons-Hainaut, Place du Parc 20, B-7000 Mons, Belgium

^bSolid State and Structural Chemistry Unit,
Indian Institute of Science, Bangalore 560012, India

ABSTRACT

The symmetrized density matrix renormalization group approach is applied within the extended Hubbard-Peierls model (with parameters U/t , V/t , and bond alternation δ) to study the ordering of the lowest one-photon (1^1B_u) and two-photon (2^1A_g) states as well as the lowest-lying triplet states in one-dimensional conjugated systems with chain lengths, N , up to $N=80$ sites. Three different types of crossovers are studied, as a function of U/t , δ , and N . The "U - crossover" and " δ - crossover" are examined for long chains, which provide a sharp contrast to the situation found previously for short chains. The "N-crossover", which only occurs for realistic intermediate correlation strength, illustrates the more localized nature of the $2A_g$ excitation relative to the $1B_u$ excitation. We also apply the quantum-chemical Pariser-Parr-Pople (PPP) model with long-range Ohno potential to the polyene molecules. We find that the $2A_g$ state is always below the $1B_u$ state for chain lengths $N=4$ to 40. Most interestingly, the gap between $2A_g$ and $1B_u$ first increases for N up to 16, then levels off, and finally starts to decrease. Thus, extrapolations to long chain based on short polyene data are hazardous.

keywords: quantum confinement, excited states, conjugated polymers, electron correlation, density matrix renormalization group, polyene, photoluminescence.

1. INTRODUCTION

Recently, much attention has focused on the luminescence properties of conjugated organic materials because of their potential for application in display devices [1]. These studies have underscored the importance of the structure of low-lying electronic excited states. Specifically, a major parameter is the relative ordering of the lowest dipole allowed singlet (1^1B_u) state and the lowest dipole forbidden singlet (2^1A_g) state, in the light of Kasha's rule which relates molecular fluorescence to the lowest excited singlet state.

It is well established that correlated electron systems behave differently from independent electron systems, especially in the case of electronic excitations. Earlier work has shown that the lowest optically forbidden excited state $2A_g$ lies below the optically allowed excited state $1B_u$ in polyene molecules [2] (thus preventing any significant luminescence in such compounds), while an independent electron model gives the opposite picture; similar results have been found by Periasamy *et al.* in the case of polycrystalline sexithienyl [3] or Lawrence *et al.* in single crystal polydiacetylene [4]. These examples serve as evident manifestation of electron correlation in conjugated molecules. The influence of electron correlation has also been considered as the main origin of lattice dimerization leading to the view that conjugated polymers are Mott insulators rather than Peierls insulators [5]. In the context of third-order nonlinear optical response (third-harmonic generation and electroabsorption) and photo-induced absorption, the role of higher-lying excited states derived from correlated electron models has also been emphasized [6]. When going from oligomer to polymer chains, continuum band states are formed, derived from the higher lying excited states of oligomers, while the $1B_u$ and $2A_g$ states keep an excitonic character.

It is also important to stress that the electronic and optical properties of conjugated oligomers and polymers differ, depending on whether the compounds are in the gas phase, solution, or the solid state [7]. The chemical environment affects the geometric structure as well as the electron correlation strength, the latter via dielectric screening [8]. Furthermore, the characteristics of the conjugation defects present in oligomers depend on chain length, which emphasizes the influence of quantum size effects [9].

In view of these features, we believe that these three factors: (i) geometric structure, (ii) strength of electron correlation, and (iii) quantum confinement, are most relevant for the study of the photo- and electro-luminescence response in organic conjugated chains.

Previous studies of the 1B/2A crossover behavior have been carried out for short chain systems. In the independent electron limit, the 2A energy is significantly higher than that of 1B due to the discreteness of the molecular orbital energy spectrum; in this zero U limit, the 2A state corresponds to single HOMO to LUMO+1 (or HOMO+1 to LUMO) excitation while 1B is a HOMO to LUMO excitation. According to previous results [10], as electron correlation U is turned on, the gap between the ground state and the 2A state narrows while the gap to the 1B state increases; the states thus cross at a given Hubbard correlation strength U_c . This, we refer to as the "U-crossover". However, for an infinite chain, the 2A and 1B states both occur at the same energy in the Hückel limit ($U=0$). If the 2A and 1B states were evolving in a manner identical to that in the short chains, these states would never cross with increasing U . Thus, for a given U , there must occur a crossover from the short chain behavior to the long chain behavior; this, we refer to as the "N-crossover".

It was noted by Soos, Ramasesha and Galvão [11] from exact diagonalization studies of short chains that a similar crossover occurred with variation of the bond-alternation parameter δ , which we refer to as the " δ crossover". The δ -crossover was studied by monitoring the optical gap and the lowest singlet-triplet (spin) gap; the critical δ_c for a given correlation strength was determined by the value of δ at which the optical gap equals twice the spin gap. These authors further described the system as behaving band-like for δ values above δ_c and correlated-like for δ values below δ_c . However, as was pointed out in Ref. [12], increasing bond alternation does not lead to the band picture, because the binding energy of the 1B exciton increases with increasing δ , an obvious indication that electron correlation increases at the same time.

In this work, we present a thorough study that encompasses the three kinds of crossovers, namely the U , N , and δ crossovers in conjugated chains, by employing the symmetrized density matrix renormalization group (SDMRG) theory. The SDMRG approach [13] is currently the most reliable many-body method for calculating the low-lying excited states with high accuracy for relatively large systems and for a wide range of model parameters. We first present an extended Hubbard-Peierls model, a physicist's general model, to study the three kinds of crossover behaviors.

We also investigate a specific case, the polyene molecules. These have been extensively studied both experimentally and quantum chemically (*ab initio* and semiempirical) [14]. Controversial results have been found in the literature concerning the ordering of $2A_g$ and $1B_u$ [15] states. Due to difficulties in treating electron correlation effects in traditional approaches, no definite results exist for polyenes with moderate sizes, *e.g.* $N \sim 20$. The limited experimental data indicate that the $2A_g$ state is below $1B_u$ from $N=6$ to $N=16$. Most interestingly, these results indicate that the gap between $1B_u$ and $2A_g$ increases as chain length increases [14,16]. A rough extrapolation by Kohler placed the $2A_g$ state energy at half that of $1B_u$ in long chain limit [17]. Experimental efforts such as two-photon absorption have been performed on trans-polyacetylene to verify this suggestion [18].

Here, we adopt the quantum-chemical model Pariser-Parr-Pople (PPP) with the long-range electron repulsion Ohno potential to calculate the low-lying excited states. Due to the almost exact nature of our approach, our results provide unambiguous theoretical evidence in terms of the evolution with chain length. In fact, we find that the $1B_u - 2A_g$ gap does increase with chain length, *only for chains shorter than $N=16$* . The gap then tends to stabilize, eventually decreases for longer chains. We will give an explanation based on the studies on the general crossover behaviors.

2. EXTENDED HUBBARD-PEIERLS MODEL AND SDMRG

The extended Hubbard-Peierls Hamiltonian reads:

$$H = -t \sum_{i,s} (1 + (-1)^i \delta) (c_{i,s}^\dagger c_{i+1,s} + h.c.) + U \sum_i n_i (n_i - 1) / 2 + V \sum_i (n_i - 1) (n_{i+1} - 1) \quad (1)$$

where δ is the dimensionless dimerization parameter, U is the on-site Hubbard repulsion, t is the nearest-neighbor hopping integral and V is the nearest-neighbor charge density-charge density interaction; n_i is the number of particle operator on site i . The δ term serves as a structural parameter in the simplest way, if we assume linear electron-lattice coupling in the static limit; as has been pointed out before, the V -term is crucial to the understanding of the optical excitation spectrum, namely the excitonic effect [19]. The present model can be regarded as the minimal correlated model for conjugated systems. Note that the meaningful phase corresponds to the BOW (bond-order wave) regime, namely, $V < U/2$ [20]. We set $V=0.4U$ without losing generality.

The density matrix renormalization group method is the most accurate numerical method for determining the ground and low-lying excited states of quasi-one-dimensional correlated electron systems with short-range interactions [20]. In the usual DMRG procedure, the good quantum numbers are the total number of particles and the total S_z component; it is thus difficult to target the singlet $1B_u$ state as there are many states that appear between it and the ground state which have different symmetry and spin. The number of these states increases with U and chain length N . As is known, DMRG works well only for low-lying states.

We have developed a symmetrized DMRG technique that exploits spin parity P , C_2 symmetry, and electron-hole symmetry J . The J and P operations hold only at half-filling. We start from a two-site system, for which exact solutions for all the states are easily obtained, along with all the fermion operator matrix representations and density matrix for a single site (half block). In Fock space, the symmetry operation is: $J_i|0\rangle=|x\rangle$, $J_i|\downarrow\rangle=(-1)^i|\downarrow\rangle$, $J_i|\uparrow\rangle=(-1)^i|\uparrow\rangle$, $J_i|x\rangle=-|0\rangle$; $P_i|0\rangle=|0\rangle$, $P_i|\downarrow\rangle=|\uparrow\rangle$, $P_i|\uparrow\rangle=|\downarrow\rangle$, $P_i|x\rangle=-|x\rangle$; where $|0\rangle$ and $|x\rangle$ represent an empty and a doubly occupied site, respectively, and site index i is relevant to the phase of e-h symmetry. Then, for the entire 4-block system, four sites right after two sites for instance, the projection operator matrix for a given irreducible representation is formed by a direct product of the four blocks:

$$J = \prod_i J_i, \quad P = \prod_i P_i, \quad \text{by virtue of } C_2 \text{ symmetry: } C_2|\mu, \sigma, \sigma', \mu\rangle = (-1)^\gamma |\mu, \sigma', \sigma, \mu\rangle, \quad \text{with phase}$$

factor $\gamma = (n_\mu + n_\sigma)(n_{\mu'} + n_{\sigma'})$, where n is the number of particles in the block. The three symmetry operators commute with each other; the generated group is an Abelian group with eight irreducible representations labeled as ${}^*A^+$, ${}^*A^-$, ${}^{\circ}A^+$, ${}^{\circ}A^-$, ${}^*B^+$, ${}^*B^-$, ${}^{\circ}B^+$, and ${}^{\circ}B^-$. The projection operator for a given irreducible representation Γ is: $P_\Gamma = \frac{1}{8} \sum_R \chi_\Gamma(R) R$,

where the R 's are the symmetry operations and χ is the character. The construction of the symmetry adapted direct product states consists in sequentially operating on each of the direct product states by the projection operator. The linear dependencies of the symmetry adapted combinations are eliminated by carrying out a Gram-Schmidt orthonormalization. In general, the operator R for a $2N+2$ system is constructed as:

$$\langle \mu, \sigma, \sigma', \mu' | R_{2N+2} | \nu, \tau, \tau', \nu' \rangle = \langle \mu | R_N | \nu \rangle \langle \sigma | R_1 | \tau \rangle \langle \sigma' | R_1 | \tau' \rangle \langle \mu' | R_N | \nu' \rangle ; \text{ in the next iteration, } R_{N+1} \text{ is formed as:}$$

$$\langle \mu, \sigma | R_{N+1} | \nu, \tau \rangle = \langle \mu | R_N | \nu \rangle \langle \sigma | R | \tau \rangle, \text{ which is renormalized by the transformation } \tilde{R}_{N+1} = O^\dagger R_{N+1} O, \text{ where } O \text{ is the truncated } N+1\text{-block density matrix eigenvectors.}$$

The coefficients of the direct product functions in the symmetrized basis form a matrix S . The Hamiltonian matrix in the direct product basis can be transformed to the Hamiltonian in the symmetrized basis by $\tilde{H}_{2N+2} = S^\dagger H_{2N+2} S$. The low-lying eigenstates of this matrix can be obtained by Davidson's diagonalization algorithm.

The $1B_u$ state is the lowest state in the subspace ${}^{\circ}B_u^-$. In fact, it is the lowest ionic state only if one employs the electron-hole symmetry. This indicates the importance of this symmetry operation. In fact, in the Hubbard model, there is a remarkable gap between the ionic space and the covalent space for all chain lengths.

Incorporating these three symmetries thus allows us to determine the $1B_u^-$ and the $2A_g^+$ state energies with unprecedented accuracy for chains of up to 80 sites [12, 13]. We choose to truncate the space of density matrix eigenstates to 100 ($m=100$) in most cases. For smaller U and δ , however, we choose a larger value of m ($=150$) in order to achieve consistent accuracy. In fact, for the ground state and the lowest triplet state, we can also apply the unsymmetrized DMRG technique because these two states are simply the lowest one in $S_z=0$ and $S_z=1$ spaces, respectively; this provides an independent check for the symmetrization scheme.

3. CROSSOVER BEHAVIORS

We contrast the "U-crossover" for short ($N=8$) and long ($N=80$) chains for fixed alternation $\delta=0.07$ in Fig. 1. It is well known that in the strong correlation limit, the $2A$ state becomes a spin excitation which is gapless in the limit $(V,\delta)=0$ and this state can be described as composed of two triplets, as early suggested by Tavan and Schulten [22]. Thus, increase in correlation strength should lead to a decrease in the $2A$ energy [22]. However, we note that in the $N=8$ chain, the two-photon state energy remains nearly constant before decreasing for values of U/t larger than 2.0. In longer chains, the $2A_g$ energy increases even more rapidly than the $1B_u$ energy with increasing correlation strength. This implies a substantial ionic contribution to the $2A_g$ state in long chains besides the covalent triplet-triplet contribution. This result constitutes the first clear illustration of the importance of quantum-size effects. We find, however, that the critical correlation strength, U_c , at

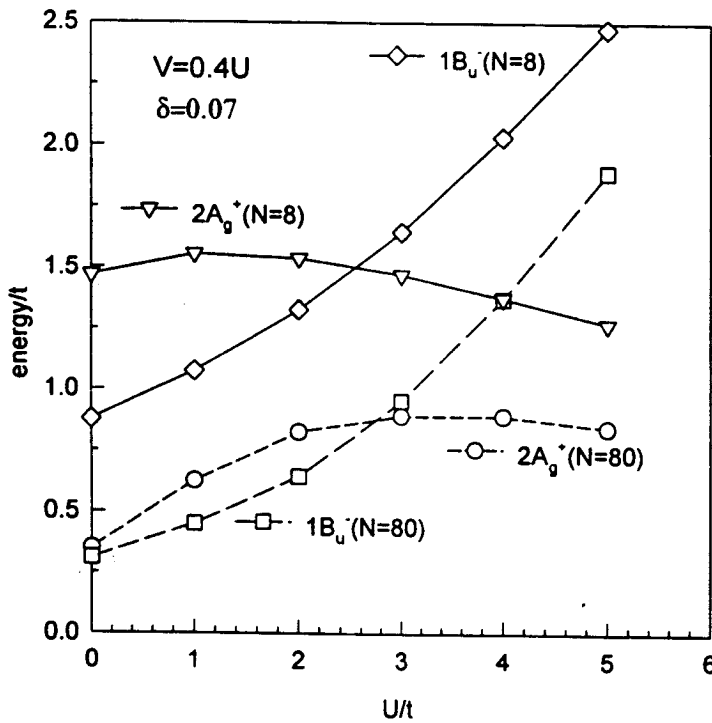


Figure 1. Crossover on U for $N=8$ and $N=80$.

which the crossover occurs is nearly independent of the chain length N ; in both $N=8$ and $N=80$ cases, U_c is around $2.5t$.

For fixed correlation strength ($U/t = 3$ and 4), we present the " δ crossover" results for $N=8$ and 80 in Fig. 2. We find that the critical δ value, δ_c , strongly depends on chain length. For $U/t=3$, the δ_c values are found to be 0.15 and 0.09 for $N=8$ and 80 , respectively; for $U/t=4$, they are 0.32 and 0.22 . Thus, δ_c has both strong N and U dependences. We also show in Fig. 2 the crossover behavior between the $1B_u$ energy and twice the lowest triplet energy, E_T . This crossover occurs at systematically smaller δ values, again emphasizing the larger ionic character present in the $2A_g$ state compared to the lowest triplet state.

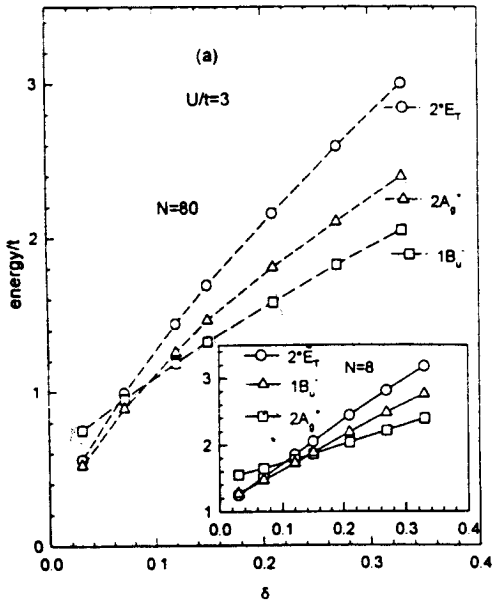


Figure 2a. δ -crossover for $U/t=3$.

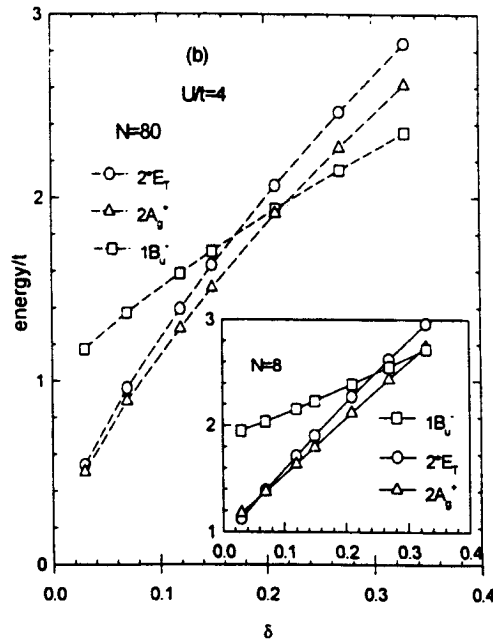


Figure 2b. δ -crossover for $U/t=4$.

Most interestingly, we find one more crossover behavior, which is the “N-crossover”, in the case of intermediate U/t and medium to large δ values. We observe that the $1B_u$ and $2A_g$ states cross over for fixed U/t and δ as a function of N , the chain length. The critical lengths are actually fairly insensitive to U and δ . In Figs. 3a ($U/t=3$, $\delta=0.12$) and 3b ($U/t=4.0$, $\delta=0.27$), we find this crossover for $N=14$ and $N=12$, respectively. This is a direct theoretical observation of quantum confinement induced crossover. It is related to the fact that the $2A_g$ excitation is more local in character with a shorter characteristic length than the $1B_u$ state. Thus, the $1B_u$ excitation is stabilized over longer length scales than the $2A_g$ excitation. This is seen as a more rapid saturation in the $2A_g$ energy compared to the $1B_u$ energy, as a function of chain length. We note that this crossover can also be seen from Fig. 2 where the δ_c values show a decrease in going from $N=8$ to $N=80$. This behavior can only exist for intermediate correlation strength: for weak correlation, there does not exist any crossover and $2A_g$ lies above the $1B_u$ state for all chain lengths as seen from Fig. 1; at large values of U/t , we are in the atomic limit, a crossover is not expected and the quantum size effects are largely suppressed. It has been widely accepted that the conjugated molecules fall in the intermediate correlation regime; thus, the confinement-induced δ crossover is realistic.

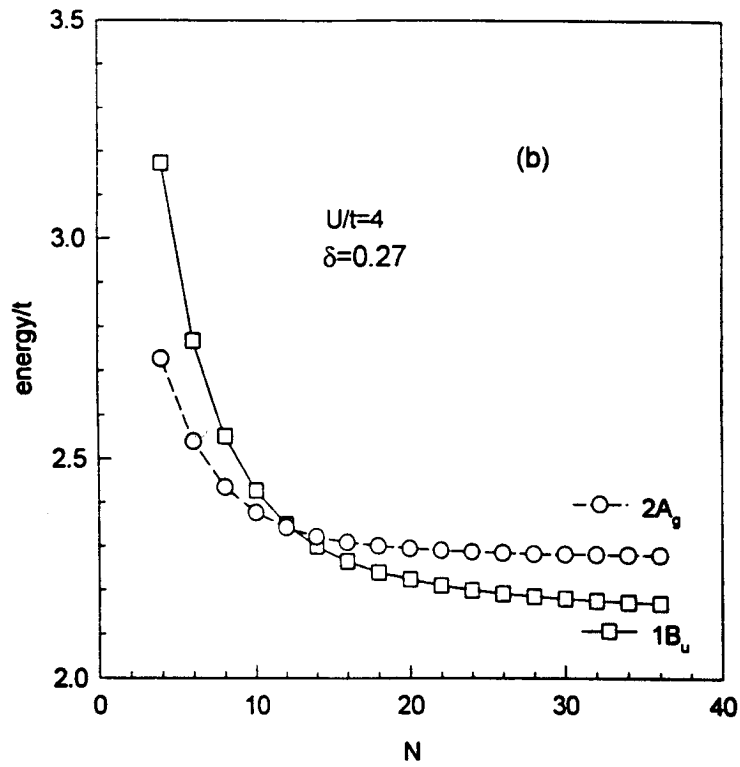


Figure 3b. N-crossover for $U/t=4$, $\delta=0.27$.

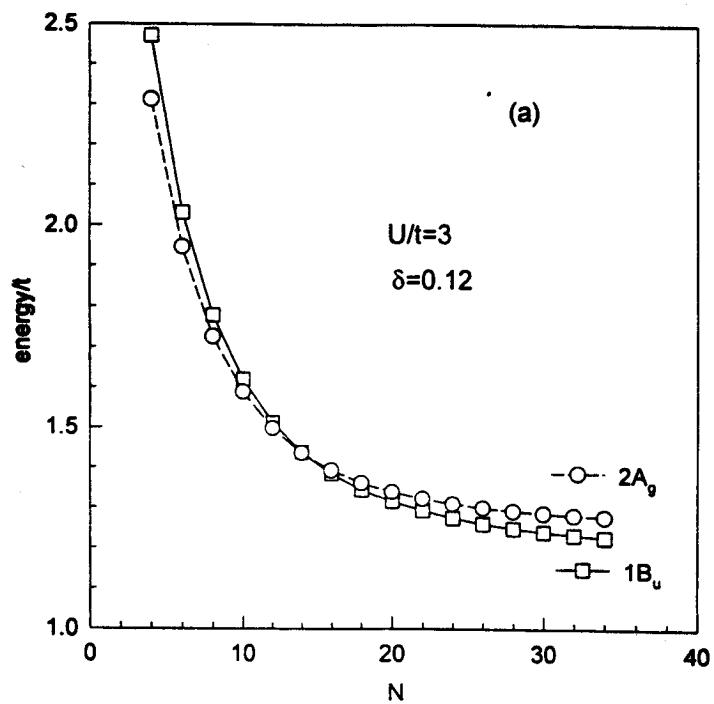


Figure 3a. N-crossover for $U/t=3$, $\delta=0.12$.

Note that we have not included the data for $N=2$. We stress that the dimer limit ($N=2$) constitutes a special case, which cannot be extrapolated to longer chains, as far as the $2A_g$ state is concerned. In the dimer limit, the exact solution for the energies of all the four states for 2 electrons (half-filling) is given below:

$$E(1A_g) = -\varepsilon, \left(\varepsilon = \frac{1}{2} \left(\sqrt{(U - V)^2 + 16t^2(1 + \delta)^2} - (U - V) \right) \right); E(\text{triplet})=0; E(1B_u)=U-V; E(2A_g)=\varepsilon+U-V.$$

In fact, $2A_g$ in the dimer is always higher than $1B_u$ regardless of the choice of parameters. In the strong correlation limit ($4t/(U-V) \rightarrow 0, \varepsilon \rightarrow 0^+$), we note that $E(1B_u)$ becomes degenerate with $E(2A_g)$ from below. From Figure 1, the “covalent” $E(2A_g)$ should come down well below $E(1B_u)$. The calculated $2A_g$ state in the dimer limit has a totally different character from that in cases $N>2$. In fact, in a two-site system, there is no space to construct two coupled triplet states; as a result, the $2A_g$ state actually corresponds to an higher-lying ionic excitonic mA_g state of the long chains, as discussed in Ref. [19]; this feature deserves further study.

3. THE PPP MODEL APPLIED TO POLYENES

In order to provide the best comparison with previous semiempirical quantum-chemical calculations on polyenes, we adopt here the Pariser-Parr-Pople Hamiltonian, with the long-range Ohno potential:

$$V(r) = \frac{U}{\sqrt{1 + (Ur / 14.397)^2}}$$

$U=11.26$ eV for carbon, r is the inter-site distance in Angstrom in all-trans polyene chains with alternating bond length of 1.36/1.45 Angstrom and 120° bond angles. This long-range term replace the nearest-neighbor V term in Hamiltonian (1) as $\sum_{i < j} V_{ij} (n_i - 1)(n_j - 1)$. The hopping t is chosen as 2.4 eV, (with $\delta=0.07$).

Even for the long range Ohno potential, the DMRG results can be also regarded as nearly exact for the ground state and a few excited states. The accuracy of the calculations is manifested in the following ways: (i) the energy of the targeted state converges with respect to increasing the dimension (the cut-off) of the truncated density matrix eigenstates, for instance, the ground state energy changes only 0.001 eV when the cut-off goes from 100 to 120 eigenstates; and (ii) the difference tends to vanish (around 10^{-5}) between 1 (exact value) and the sum of the eigenvalues of the truncated density matrix. This is a natural way to track the precision of a DMRG calculation, as suggested by White [20].

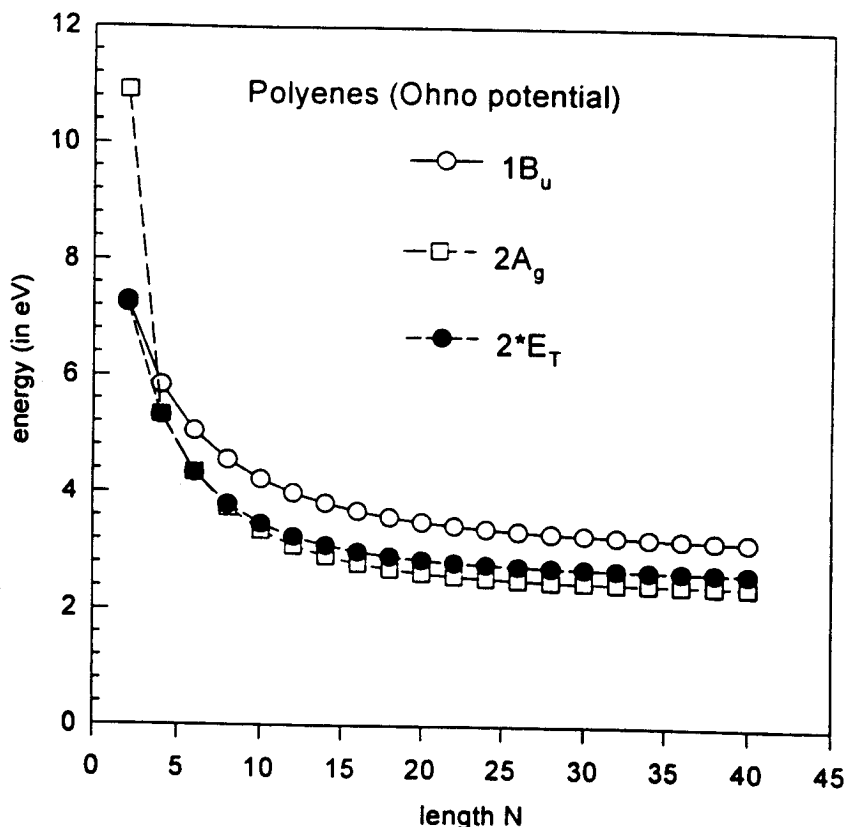


Figure 4. Excited states of polyenes.

The PPP evolution with chain length of the lowest-lying excited states of polyenes are depicted in Figure 4. For the chosen set of parameters (which is widely employed in the literature), there does not exist any N-crossover; for all systems, the covalent $2A_g$ state is always below $1B_u$. Note that the “exotic” $2A_g$ state for $N=2$ is shown in Fig. 4; it is much higher in energy than both $1B_u$ and twice the lowest triplet state. Most interestingly, we find that the difference between $1B_u$ and $2A_g$ increases with chain length in the short-chain regime, then levels off, and finally starts decreasing (see Figure 5). In Table 1, we present the DMRG results which we believe represent the most accurate theoretical calculations to date.

The $1B_u$ - $2A_g$ gap increase in the short-chain regime had been long observed in experiments. Based on such data, Kohler developed an extrapolation model and concluded that in the long-chain limit, the $2A_g$ state energy should appear at only half that of $1B_u$. Since the model is not size-consistent and the data are limited to short chains, it is not unexpected that such an extrapolation is in sharp contradiction with the results of our accurate calculations. In fact, if we extrapolate to polyacetylene our data on the long polyenes, the $1B_u$ and $2A_g$ states energies are found to be 2.92 eV and 2.31 eV, respectively (the difference thus being 0.61 eV). The 2.92 eV value for the $1B_u$ energy is about 1 eV higher than the experimental result for polyacetylene in solid state. This discrepancy can be ascribed to solid state polarization effects or to the inadequacy of molecular parameters for solids. The solid-state polarization effect should be smaller for the $2A_g$ state than for $1B_u$, because the former is “covalent” while the latter is ionic. Another aspect is that the solid-state polarization affects more an anion or cation state (thus, the continuum bandgap) than the $1B_u$ state, which is a bound state of two opposite charges. This argument leads Moore and Yaron to stress the decreased polarization effect on the $1B_u$ exciton binding energy [24]; similarly, this effect should also reduce the $1B_u$ - $2A_g$ value from gas phase to solid.

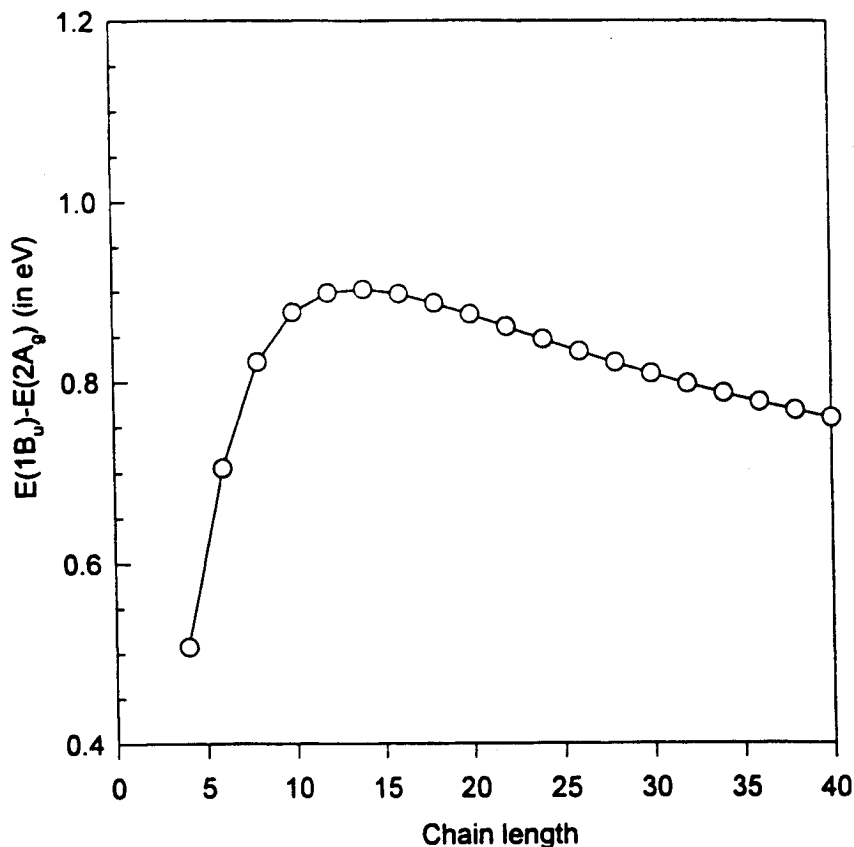


Figure 5. Evolution of $E(1B_u) - E(2A_g)$ with N .

Table 1. Symmetrized DMRG results for the lowest-lying excited state energies (in eV) of polyenes with 4 to 30 carbons. The PPP parameters are $t = -2.4$ eV, $\delta = 0.07$, and $U = 11.26$ eV. All the values correspond to the vertical transition energies from the $1A_g$ ground state.

N	4	6	8	10	12	14	16	18	20	22	24	26	28	30
$1B_u$	5.835	5.050	4.558	4.226	3.992	3.819	3.689	3.588	3.508	3.445	3.393	3.351	3.316	3.287
$2A_g$	5.328	4.345	3.736	3.350	3.093	2.916	2.791	2.701	2.634	2.584	2.547	2.518	2.496	2.478
1T	2.655	2.167	1.896	1.731	1.623	1.549	1.497	1.458	1.429	1.407	1.390	1.376	1.364	1.355

4. SYNOPSIS

To conclude, we have employed the accurate numerical density matrix renormalization group technique with symmetry adaptation to study the ordering of the lowest one-photon and two-photon states in conjugated oligomers and polymers within an extended Hubbard-Peierls model. Three kinds of crossover, namely a “U-crossover”, a “ δ -crossover”, and a “N-crossover”, have been demonstrated. The “N-crossover” is related to quantum finite size effects and crucially depends on the characteristic length of the excitations.

In addition to these general crossover behaviors, we have shown that when a long-range Ohno potential is applied to polyene molecules, the evolution of the $2A_g$ and $1B_u$ state energies as a function of chain length, is different from the extrapolation based on a few experimental data for short chains. We find that the gap between $1B_u$ and $2A_g$ first increases for $N < 14$ carbons, then starts decreasing for $N > 16$.

ACKNOWLEDGMENTS

This work is partly supported by the Belgian Prime Minister Services for Scientific, Technical, and Cultural Affairs (Interuniversity Attraction Pole 4/11 in Supramolecular Chemistry and Catalysis), FNRS/FRFC, and an IBM Academic Joint Study. The work in Bangalore is partly supported by the Jawaharlal Nehru Center for Advanced Scientific Research.

REFERENCES

- [1] J. H. Burroughes, D. D. C. Bradley, A. R. Brown, R. N. Marks, K. Mackay, R. H. Friend, P. L. Burn, and A. B. Holmes, *Nature* **347**, 539 (1990); G. Gustafsson, Y. Cao, G. M. Treacy, F. Klavetter, N. Colaneri, and A. J. Heeger, *Nature* **357**, 477 (1992).
- [2] B. S. Hudson and B. E. Kohler, *Chem. Phys. Lett.* **14**, 229 (1972); *J. Chem. Phys.* **59**, 4984 (1973).
- [3] N. Periasamy, R. Danieli, G. Ruani, R. Zamboni, and C. Taliani, *Phys. Rev. Lett.* **68**, 919 (1992).
- [4] B. Lawrence, W. E. Torruellas, M. Cha, M. L. Sundheimer, G. I. Stegeman, J. Meth, S. Etemad, and G. Baker, *Phys. Rev. Lett.* **73**, 597 (1994).
- [5] S. Mazumdar and D. K. Campbell, *Phys. Rev. Lett.* **55**, 2067 (1985); C. Q. Wu, X. Sun, and K. Nasu, *Phys. Rev. Lett.* **63**, 2534 (1989).
- [6] J. M. Leng, S. Jeglinski, X. Wei, R. E. Benner, Z. V. Vardeny, F. Guo, and S. Mazumdar, *Phys. Rev. Lett.* **72**, 156 (1994); F. Guo, M. Chandross, and S. Mazumdar, *Phys. Rev. Lett.* **74**, 2096 (1995); S. N. Dixit, D. Guo, and S. Mazumdar, *Phys. Rev. B* **43**, 6781 (1991).
- [7] O. Dippel, V. Brandl, H. Bäessler, R. Danieli, R. Zamboni, and C. Taliani, *Chem. Phys. Lett.* **216**, 418 (1993).
- [8] S. R. Marder, C. B. Gorman, F. Meyers, J. W. Perry, G. Bourhill, J. L. Brédas, and B. M. Pierce, *Science* **265**, 632 (1994).
- [9] J. L. Brédas and A. J. Heeger, *Chem. Phys. Lett.* **154**, 56 (1989).
- [10] a) G. W. Hayden and E. J. Mele, *Phys. Rev. B* **34**, 5484 (1986); b) D. Baeriswyl, D. K. Campbell, and S. Mazumdar, in *Conjugated Conducting Polymers*, edited by H. Kiess, (Springer-Verlag, Berlin, 1992), and references therein.
- [11] Z. G. Soos, S. Ramasesha, and D. S. Galvão, *Phys. Rev. Lett.* **71**, 1609 (1993).
- [12] Z. Shuai, S. K. Pati, W. P. Su, J. L. Brédas, and S. Ramasesha, *Phys. Rev. B* (June 1997).
- [13] S. Ramasesha, S. K. Pati, H. R. Krishnamurthy, Z. Shuai, and J. L. Brédas, *Phys. Rev. B* **54**, 7598 (1996).
- [14] B. Hudson, B. E. Kohler, and K. Schulten, in *Excited States*, ed. by E. C. Lim (Academic, New York, 1982), Vol. 6, p. 1.
- [15] R. J. Cave and E. R. Davidson, *J. Phys. Chem.* **92**, 2173 (1988).
- [16] B. E. Kohler, *J. Chem. Phys.* **93**, 5838 (1990).
- [17] B. E. Kohler, *J. Chem. Phys.* **88**, 2788 (1988).
- [18] C. Halvorson and A. J. Heeger, *Chem. Phys. Lett.* **216**, 488 (1993).
- [19] D. Guo, *et al.*, *Phys. Rev. B* **48**, 1433 (1993).
- [20] S. Mazumdar and D. K. Campbell, *Phys. Rev. Lett.* **55**, 2067 (1985); see also Ref. [10b].
- [21] S. R. White, *Phys. Rev. Lett.* **69**, 2863 (1992); *Phys. Rev. B* **48**, 10345 (1993).
- [22] P. Tavan and K. Schulten, *Phys. Rev. B* **36**, 4337 (1987); *J. Chem. Phys.* **85**, 6602 (1986).
- [23] D. Mukhopadhyay, G. W. Hayden, and Z. G. Soos, *Phys. Rev. B* **51**, 9476 (1995).
- [24] E. Moore, B. Gherman, and D. Yaron, *J. Chem. Phys.* **106**, 4216 (1997); E. Moore and D. Yaron, *Synth. Met.* **85**, 1023 (1997).